Mean-field equations for configurational kinetics of alloys at arbitrary degree of nonequilibrium

V. G. Vaks, S. V. Beiden, and V. Yu. Dobretsov
Kurchatov Institute, Russian Research Center, 123182 Moscow, Russia

(Submitted 6 December 1994)
Pis'ma Zh. Eksp. Teor. Fiz. **61**, No. 1, 65–70 (10 January 1995)

The mean-field approximation is applied to the master equation describing the time evolution of alloy states to obtain kinetic equations for concentrations at an arbitrary degree of nonequilibrium. The application of these equations to several problems of phase transformations is discussed. © *1995 American Institute of Physics.*

Problems of structural evolution of nonequilibrium alloy states attract much attention. Theoretically, they are studied using either approximate kinetic equations[1–7] (AKE) for the local concentration or mean occupation number $c_i = c(\mathbf{r}_i, t)$ at the lattice site i (say, for A atoms in the binary (A–B) alloy), or direct simulation, e.g., Monte Carlo (MC) methods.[8–11] The approximate kinetic equations seem to be more transparent and universal than simulation methods, and many new qualitative results in this field[1–4] were obtained using AKE. However, the currently used phenomenological forms of AKE are based on Onsager-type linear relations[12] between time derivatives, dc_i/dt, and thermodynamic driving forces, $\partial F/\partial c_j$ (where F is the free energy of an inhomogeneous alloy), which hold only for near-equilibrium states. Thus, application of these AKE to states far from equilibrium, such as those obtained by deep quenching, transient states at spinodal decomposition (SD), etc. can hardly be justified, while kinetic phenomena just in these states seem to attract most interest.[3,4,12]

To investigate these phenomena more consistently, we use the fundamental master equation which determines the probability $P\{n_i, t\}$ of finding the set of occupation numbers $\{n_i\}$ (where $n_i = 1$ if atom A is at site i and $n_i = 0$ otherwise) in terms of microscopic probabilities for intersite atomic jumps.[7] To use this equation, we apply the mean-field approximation (MFA) which was earlier developed for description of steady states in irradiated alloys.[7] We assume that interatomic potentials v_{ij} obey conditions for the applicability of MFA; i.e., their interaction range includes a sufficiently large number of sites $N_0 \gg 1$, which for actual alloys can be true even quantitatively.[4]

Following Ref. 7, we multiply the master equation by the operators n_i, $n_i n_j$, etc. and average these relations. For inhomogeneous alloys under consideration such averaging, e.g., that for $\langle n_i \rangle = c_i = c(\mathbf{r}_i, t)$, has a clear meaning only if the characteristic lengths l for space variation of c_i exceed the intersite distance a. Since l is usally not lower than the interaction radius r_0, which is assumed to be large, the above condition in our case is satisfied. The resulting equations for $\langle n_i \rangle$ and the correlators of the fluctuations $K_{i\ldots j} = \langle (n_i - c_i) \ldots (n_j - c_j) \rangle$ in the main approximation in $1/N_0$ decouple[7] and can be written explicitly. Using for the thermally activated intersite jumps a "direct-jump"

model described in Refs 5 and 7, we obtain the mean-field kinetic equation for the A–B alloy

$$dc_i/dt=\sum_s \gamma_{is}(c_i' c_s e^{\varphi_s^A+\varphi_i^B}-c_s' c_i e^{\varphi_i^A+\varphi_s^B}). \tag{1}$$

Here $\gamma_{is}=\gamma_{si}$ is the c_i-independent part of the jump probability, $c_i'=1-c_i$, $\varphi_i^p=\beta(v^p c)_i$, $\beta=1/T$ is the reciprocal temperature, $(v^p c)_i=\Sigma_j v_{ij}^p c_j$ is the MFA potential acting on a p-species atom at site i, and v_{ij}^A and v_{ij}^B are related to the configurational potential $v=V^{AA}+V^{BB}-2V^{AB}$ and the "asymmetric" potential $v=V^{AA}-V^{BB}$ as $v^A=\frac{1}{2}(u+v)$, $v^B=\frac{1}{2}(u-v)$.

Writing the reduced MFA free energy $f=\beta F$ for an inhomogeneous alloy as

$$f=\sum_i (c_i \ln c_i+c_i' \ln c_i')+\frac{1}{2}\sum_{ij} \beta v_{ij} c_i c_j, \tag{2}$$

we can express Eq. (1) in the form

$$dc_i/dt=\sum_s A_{is}[\exp(\partial f/\partial c_s)-\exp(\partial f/\partial c_i)], \tag{3}$$

where $A_{is}=A_{si}>0$. For fully equilibrium states all derivatives $f_i=\partial f/\partial c_i$ are equal to the chemical potential μ_s. The right-hand side of Eq. (3) therefore vanishes. For the near-equilibrium states we can expand the right side in powers of f_s-f_i, which converts it into the Onsager form $\Sigma_s L_{is} f_s$ used in Refs. 3 and 4. We see that this linearized equation ignored not only higher powers of f_s-f_i, but also the c_i-dependence of the kinetic coefficients L_{ij}. For states far from equilibrium, e.g., at deep quenching or at late stages of SD (when the factors c_i or c_i' in (1) become close to zero), the latter can lead to significant errors.

Multiplying Eq. (1) by f_i, summing over i, and denoting $\exp(f_i)$ as ξ_i, we obtain an analog of the H-theorem for alloys (earlier discussed by Penrose):[6]

$$df/dt=\frac{1}{2}\sum_{is} A_{is}(\xi_s-\xi_i)\ln(\xi_i/\xi_s)\leqslant 0. \tag{4}$$

Relations (1)–(4) are immediately generalized to many-component alloys. In particular, Eqs. (1) and (2) for them take the form

$$dc_{pi}/dt=\sum_{qs} \gamma_{is}^{pq}[\exp(f_{ps}+f_{qi})-\exp(f_{pi}+f_{qs})], \tag{5}$$

$$f=\sum_{pi} c_{pi} \ln c_{pi}+\frac{1}{2}\sum_{pi,qj} \beta v_{ij}^{pq} c_{pi} c_{qj}. \tag{6}$$

Here $c_{pi}=\langle n_{pi}\rangle$ is the mean occupation number of site i by a p-species atom, and f_{pi} is the formal partial derivative $\partial f/\partial c_{pi}$ of the function (6), disregarding the normalizing condition $\Sigma_p c_{pi}=1$. Equation (5) can be applied, in particular, to the alloy A–B, where

the vacancies (ABv-alloy) are treated as a three-component alloy. Since the intersite jumps in alloys are mainly realized via vacancies, Eq. (5) enables us to find the expressions for the effective "direct jump probabilities" γ in (1) in terms of the microscopic vacancy–atom jump probabilities (see the discussion below).

The intersite jumps in Eqs. (1) and (5) occur mainly between nearest or next-nearest sites i and s. For disordered alloys the relevant values of c_i and c_s in our case, as mentioned above, should be close to each other. Expanding the differences $c_s - c_i$ in powers of $\mathbf{r}_{si}\Delta c$, where $\mathbf{r}_{si} = \mathbf{r}_s - \mathbf{r}_i$, we obtain a continuous version of Eq. (1)

$$\partial c_i/\partial t = \operatorname{div}\{M(c)[\nabla c/cc' + \nabla(\beta v c)_i]\}. \tag{7}$$

Here $c = c_i$, $M(c) = \gamma cc' e^{\beta(uc)_i}$ is the c_i-dependent mobility and the tensor γ is $\frac{1}{2}\Sigma_s \gamma_{is}\mathbf{r}_{is}\mathbf{r}_{is}$ (it becomes a scalar for cubic lattices). If we assume that the characteristic length l for the space variations of c_i exceeds not only a, but also the interaction radius r_0, we can approximate the last term Eq. (7) as $(vc)_i \simeq v_0 c + \epsilon\Delta c$, where $v_0 = \Sigma_j v_{ij} = -4T_0$ determines the critical temperature T_0 for SD, and ϵ is $\frac{1}{6}r_0^2 v_0$ (for cubic lattices). Linearizing (7) in the deviations $c_i - c_0$ from the initial constant value c_0, we obtain the Cahn–Hillard (CH) equation[1] which describes the early stages of SD, with the Martin expression[6] for the mobility $M_{\mathrm{CH}} = M(c_0)$. At later stages of SD concentrations c_i approach their "liquid" or "gas" values at the binodal curve, while the interface widths l decrease and become $\sim r_0$. To describe these stages of SD and also the effects of long-range elastic interactions; for which the inequality $l \gg r_0$ is violated,[4] we should therefore employ the full equation (7).

Generalizing (7) for the m-component alloy, we obtain an analogous set of equations for $m-1$ independent concentrations $c_{\mathrm{p}i}$. For the ABv-alloy, we find that c_{vi} is quite small and thus its time variations adiabatically follow fast those of $c_{\mathrm{A}i}$, so $c_{\mathrm{v}i}$ is determined by Eq. (5) with p=v and $c_{\mathrm{v}i} = 0$. The resulting equation for $c_i = c_{\mathrm{A}i}$ will then differ from Eq. (7) only by a factor $\tilde{\gamma}^{\mathrm{AB}}/\gamma$ on the right-hand side, where $\tilde{\gamma}^{\mathrm{AB}} \propto c_{vi}$ is determined by the "series-connection" relation for mobilities

$$\tilde{\gamma}^{\mathrm{AB}} cc' e^{\beta(uc)_i} = (1/M_{\mathrm{Av}} + 1/M_{\mathrm{Bv}})^{-1}. \tag{8}$$

Here $M_{\mathrm{pq}} = \gamma^{\mathrm{pv}} c_{\mathrm{p}} c_{\mathrm{q}} e^{\varphi_{\mathrm{p}} + \varphi_{\mathrm{q}}}$, $c_{\mathrm{p}} = c_{\mathrm{p}i}$, $\varphi_{\mathrm{p}} = \beta\Sigma_{\mathrm{q}j} v_{ij}^{\mathrm{pq}} c_{\mathrm{q}j}$, and γ^{pv} is defined analogously to γ after Eq. (7) substituting γ_{is} by $\gamma_{is}^{\mathrm{pv}}$. However, the compact Eq. (7), with substitution of M by Eq. (8), can be used only in the linear approximation in ∇c, since $\tilde{\gamma}^{\mathrm{AB}}$ in (8) depends on c_i.

For the ordered alloy with ν different sublattices α the averages $\langle n_{\mathrm{p}i}^{\alpha}\rangle = c_{\mathrm{p}i}^{\alpha}$ are taken for each sublattice separately. Thus, the site numbers i and j in Eqs. (1)–(6) are replaced by pairs of indices: $i \to i\alpha$, $v_{ij}^{\mathrm{pq}} \to v_{ij}^{\mathrm{pq},\alpha\beta}$, etc., where i or j now number different ν atomic cells. Writing Eq. (5) in terms of the mean cell concentrations $c_{\mathrm{p}i}$ and $\nu-1$ order parameters $\eta_{\mathrm{p}i}^{\lambda}$, we obtain a generalization of the Allen–Cahn equation[2] for the kinetics of alloy ordering, which will be discussed elsewhere.

Equations (1)–(8) can be applied to most problems of nonlinear kinetics of alloys. Below we discuss several examples.

1. Nonlinear concentration waves at the first stage of SD. According to the linearized CH equation[1] after a quench of an alloy below the spinodal curve (SC) there is

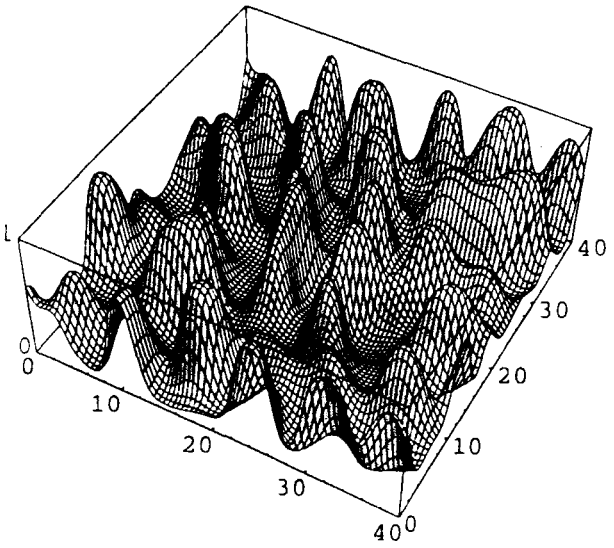

FIG. 1. Profile of the concentration $c(\mathbf{r})$ at spinodal decomposition in the 2D model described in the text for the following parameter values: $c_0=0.35$, $T=0.4T_0$, $u=0$, and $t'=10$.

a wave-like distribution of concentrations $c(\mathbf{r},t)$, which has a characteristic wavelength $2\pi/k_{\mathrm{CH}}$ and its amplitudes increase with a characteristic time $t_{\mathrm{CH}}\sim k_{\mathrm{CH}}^{-2}$, where k_{CH} is the CH wave number (which decreases when the initial concentration c_0 approaches (SC). However, it was argued that nonlinear effects neglected in the CH theory can suppress the development of pronounced CH waves.[12] From the other side, MC simulations using short-range potentials produce for first stages of SD random clusters rather than wave-like patterns.[8,9] It was also shown[10] that with an increase in the interaction range r_0 some MC results near SC converge to those of MFA. However, even for long-range potentials the importance of the above-mentioned nonlinear effects seems to remain unclear.[11]

To investigate this point and other problems of SD, we performed two-dimensional (2D) simulations based on Eq. (7). We approximated the sums $(vc)_i$ by integrals and assumed $v(r)$ to be Gaussian: $v(\tau)= - A\exp(-r^2/2\sigma^2)$ assuming $\sigma \gg \alpha$, while the constant A is proportional to the MFA critical temperature T_0. The asymmetric potential u was assumed to be less long-range than v. Thus we set $(uc)_i \simeq u_0 c_i$. Simulations were made at a square lattice $40\sigma\times 40\sigma$ with periodic boundary conditions, using the dimensionless time variable $t'=t\gamma\sigma^{-2}$. The as-quenched distribution $c(\mathbf{r},0)$ was characterized by its mean value c_0 and by small random fluctuations. Equation (7) was solved by using the Runge–Kutta method.

For all the states c_0, T within SC after times $t_1\sim k_{\mathrm{CH}}^{-2}$ we observed a pronounced wave-like structure with $\lambda\sim 2\pi/k_{\mathrm{CH}}$. It retained its features well within the nonlinear region, up to the next, coarsening stage of SD. It is illustrated by Fig. 1, while Fig. 3b shows the next stage. Thus, the nonlinear effects do not destroy the qualitative features of the CH picture for the first stage of SD at least for the long-range interactions considered by us.

2. "Bridge" mechanism for droplet coalescence. Until recently, only two coarsening mechanisms were discussed for the droplet phase separation (i) Lifshitz–Slyozov

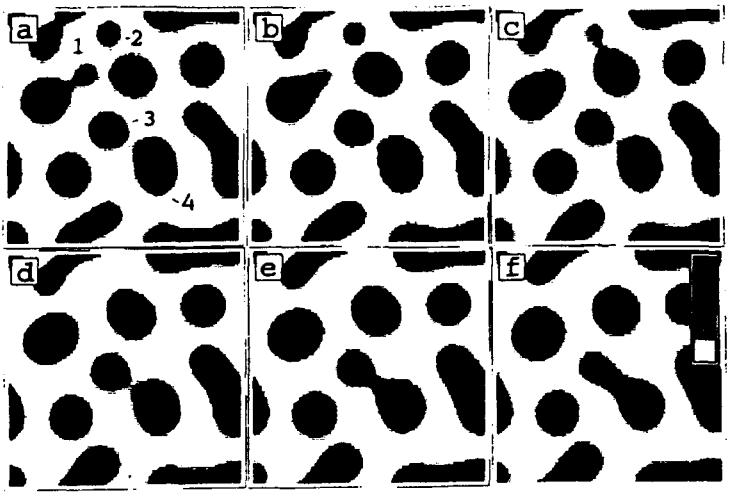

FIG. 2. Temporal evolution of the concentration $c(\mathbf{r})$ for the 2D model described in the text at $c_0=0.35$, $T=0.4T_0$, $\mu=0$ and the following t': (a) 120, (b) 130, (c) 140, (d) 160, (e) 180, and (f) 200. The insert in Fig. 2(f) shows the relation between darkness and c values which vary between 0 and 1 from bottom to top.

(LS) evaporation-condensation mechanism for separated droplets in which bigger droplets grow at the expense of evaporation of smaller ones,[14] and (ii) Binder and Stauffer mechanism[9,11] for droplet coalescence caused by their thermal diffusion without any interaction. Recently, Tanaka[13] observed peculiar effects of inter-droplet interaction under their coalescence during SD in a 2D fluid mixture, which he attributed to droplet diffusion in liquids.

In our simulations we observed similar effects for the solid alloy model, in which we see no diffusion of droplets as whole, but rather a strong dynamic coupling of diffusion fluxes around droplets. This new mechanism of coalescence (called the "bridge" mechanism) is illustrated in Fig. 2. It dominates the first stage of coarsening of the droplet pattern at intermediate c_0 vales (for example, for $t'=20$–500 at $c_0=0.35$ we have $u=0$) before the LS mechanism becomes effective.

Figures 2a–2f illustrate two main versions of the bridge mechanism: (i) that for droplets 1 and 2, when a smaller droplet is consumed by its bigger neighbor(s) which pull it over the bridge formed by diffusion fluxes, and (ii) that for droplets 3 and 4 of similar size, when the "bridge" remains a considerable time (e.g., $\Delta t'\sim 100$ for droplets 3 and 4) before its density begins to sharply rise and its droplets coalesce. These effects seem to be rather similar to those shown by Tanaka[13] in his Figs. 1 and 4.

3. Effect of A–B asymmetry of mobilities in the A–B alloy on SD. Such asymmetry is always present in real alloys but is usually disregarded in theoretical treatments. In our model it is described by the MFA value u_0 of the asymmetric potential u. The presence of the factor $\exp(\beta u_0 c)$ in the mobility results, first in a c-dependent change of the time scale, i.e., slowing down the kinetics at $u<0$ and speeding it up at $u>0$. Secondly, this factor changes the relative importance of the LS and the droplet coagulation

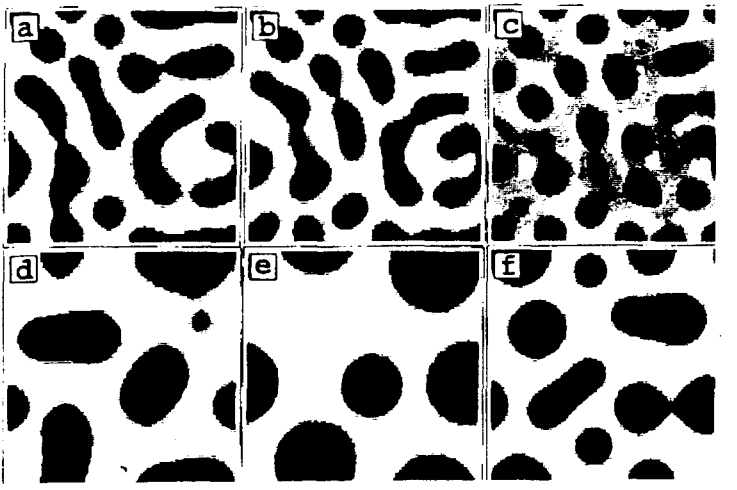

FIG. 3. Same as in Fig. 2 at $c_0=0.35$, $T=0.4T_0$, and the following values (u_0,t'): (a) $-2T_0$, 200; (b) 0, 20; (c) $2T_0$, 2.4; (d) $-2T_0$, 1230; (e) 0, 5000; and (f) $2T_0$, 16.5.

mechanisms of coarsening. Since coagulation proceeds via the bridge mechanism which corresponds to noticeable values $c\sim 0.1-0.2$ in the bridge region, the negative u lead to a suppression of this mechanism with respect to the LS mechanism, as the latter is determined by diffusion in the "gas" region $c\ll 1$, where the suppression is small. At positive u the situation reverses. For example, at $c_0=0.35$, $t=0.4T_0$, and $u_0=-2T_0$ the coarsening proceeds via the evaporation of and coalescence of two droplets (of the total of 11) during $t'=250-2500$; at $u_0=0.7$ thirteen droplets coalesce and two evaporate during $t'=50-5000$; and at $u_0=2T_0$, 13 of 18 droplets coagulate and no droplets evaporate during $t'=3-35$. Figures 3a–3c illustrate the effect of u on the formation of droplet pattern; Figs. 3d and 3f show typical coarsening mechanisms for $u_0=-2T_0$ and $u_0=2T_0$, respectively, and Fig. 3e shows an advanced stage of coarsening when the LS mechanism dominates.

This work was initiated by stimulating discussions with G. Martin. This work was supported by the International Science Foundation under Grant MQA000, and by the Russian Fund for Fundamental Research under Grant 93-02-14776.

[1] J. V. Cahn, Acta Metall. **9**, 795 (1961).
[2] S. M. Allen and J. V. Cahn, *ibid* **27**, 1085 (1979).
[3] L.-Q. Chen and A. G. Khachaturyan, Phys. Rev. B **44**, 4681 (1991).
[4] S. Semenovskaya and A. G. Khachaturyan, Phys. Rev. Lett. **67**, 2223 (1991).
[5] G. Martin, Phys. Rev. B **41**, 2279 (1990).
[6] O. Penrose, J. Stat. Phys. **63**, 975 (1991).
[7] V. G. Vaks and S. V. Beiden, Zh. Exp. Teor. Fiz. **105**, 1017 (1994) [JETP **78**, 546 (1994)].
[8] M. Rao *et al.*, Phys. Rev. B **13**, 4328 (1976).
[9] K. Binder and D. Stauffer, Adv. Phys. **25**, 343 (1976).
[10] D. W. Heermann *et al.*, Phys. Rev. Lett. **49**, 1262 (1982).
[11] J. D. Gunton *et al.*, *Phase Transitions and Critical Phenomena*, ed. by C. Domb and J. H. Lebowitz (Academic, London, 1983), Vol. 8, p. 269.

[12] A. G. Khachaturyan, *Theory of Phase Transformations and Structure of Solid Solutions*, Nauka, Moscow, 1974.
[13] H. Tanaka, Phys. Rev. Lett. **72**, 1702 (1994).
[14] I. M. Lifshitz and V. V. Slyozov, J. Phys. Chem. Solids **19**, 35 (1961).

Published in English in the original Russian journal. Reproduced here with stylistic changes by the Translation Editor.